Drosophila melanogaster alcohol dehydrogenase: mechanism of aldehyde oxidation and dismutation

Jan-Olof WINBERG*[1] and John S. McKINLEY-McKEE†

*Biochemistry Department, Institute of Medical Biology, University of Tromsø, 9037 Tromsø, Norway, and †Biochemical Institute, University of Oslo, P.B. 1041 Blindern, 0316 Oslo, Norway

Drosophila alcohol dehydrogenase (Adh) catalyses the oxidation of both alcohols and aldehydes. In the latter case, the oxidation is followed by a reduction of the aldehyde, i.e. a dismutation reaction. At high pH, dismutation is accompanied by a small release of NADH, which is not observed at neutral pH. Previously it has been emphasized that kinetic coefficients obtained by measuring the increase in A_{340}, i.e. the release of NADH at high pH is not a direct measure of the aldehyde oxidation reaction and these values cannot be compared with those for alcohol dehydrogenation. In this article we demonstrate that this is not entirely true, and that the coefficients ϕ_B and ϕ_{AB}, where B is the aldehyde and A is NAD^+, are the same for a dismutation reaction and a simple aldehyde dehydrogenase reaction. Thus the substrate specificity of the aldehyde oxidation reaction can be determined by simply measuring the NADH release. The coefficients for oxidation and dehydrogenation reactions (ϕ_{0d} and ϕ_{Ad} respectively) are complex and involve the constants for the dismutation reaction. However, dead-end inhibitors can be used to determine the quantitative contribution of the kinetic constants for the aldehyde oxidation and reduction pathways to the ϕ_{0d} and ϕ_{Ad} coefficients. The combination of dead-end and product inhibitors can be used to determine the reaction mechanism for the aldehyde oxidation pathway. Previously, we showed that with *Drosophila* Adh, the interconversion between alcohols and aldehydes followed a strictly compulsory ordered pathway, although aldehydes and ketones formed binary complexes with the enzyme. This raised the question regarding the reaction mechanism for the oxidation of aldehydes, i.e. whether a random ordered pathway was followed. In the present work, the mechanism for the oxidation of different aldehydes and the accompanying dismutation reaction with the slow alleloenzyme (Adh^S) from *Drosophila melanogaster* has been studied. To obtain reliable results for the liberation of NADH during the initial-rate phase, the reaction was measured with a sensitive recording filter fluorimeter, and the complexes formed with the different dead-end and product inhibitors have been interpreted on the basis of a full dismutation reaction. The results are only consistent with a compulsory ordered reaction mechanism, with the formation of a dead-end binary enzyme–aldehyde complex. Under initial-velocity conditions, the rate of acetate release was calculated to be larger than 2.5 s^{-1}, which is more than ten times that of NADH. The substrate specificity constant (k_{cat}/K_m or $1/\phi_B$) with respect to the oxidation of substrates was propan-2-ol > ethanol > acetaldehyde > trimethylacetaldehyde.

INTRODUCTION

The gene for alcohol dehydrogenase (Adh) has been cloned and sequenced from various *Drosophila* species, and the enzyme has been purified and biochemically characterized from some of these species (for review, see [1–3]). The Adh enzyme catalyses the interconversion of alcohols and their corresponding aldehyde/ketone products (eqn. 1) and it is also capable of oxidizing aldehydes to the corresponding acids [4–8], in a reaction which is essentially irreversible (eqn. 2).

$$\text{aldehyde/ketone} + NADH + H^+ \leftrightarrow NAD^+ + \text{alcohol} \quad (1)$$

$$\text{aldehyde} + H_2O + NAD^+ \rightarrow \text{carboxylate}^- + NADH + 2H^+ \quad (2)$$

$$2\ \text{aldehyde} + H_2O \rightarrow \text{carboxylate}^- + \text{alcohol} + H^+ \quad (3)$$

Drosophila Adh is a dimer of M_r 54800, consisting of two identical subunits [1–3], that belongs to the 'short-chain' dehydrogenase family [9,10] which lack metal ions in their active site. Site-directed mutagenesis showed that Tyr-152 and Lys-156, in contrast to the two cysteine residues in the enzyme, were essential for activity [11–13]. Binding of alcohol and alcohol-competitive inhibitors to the slow alleloenzyme from *Drosophila melanogaster* (Adh^S) was dependent on a residue in the active site, which showed a pK value of about 7.6 in the binary enzyme–NAD^+ complex [14]. This indicated that Tyr-152 could be the residue which interacts with the hydroxyl group in the alcohol and hence takes over the function of zinc in horse liver Adh [14,15].

Based on studies using alternate substrates, dead-end and product inhibitors [3,16], it has been shown that *Drosophila* Adhs follow a compulsory ordered mechanism in the interconversion of alcohols and their corresponding aldehyde and ketone products (Scheme 1, lower pathway). Eqn. (4) shows the rate expression for the liberation of Q in Scheme 1, with A, B, P, Q and S present.

$$v/e = \frac{k_1k_3k_5k_7(k_{10}+k_{11})AB - k_2k_4k_6k_8(k_{10}+k_{11})PQ}{\begin{aligned}&k_2k_7(k_4+k_5)(k_{10}+k_{11}) + k_2k_{10}k_{12}(k_4+k_5)S + k_2k_4k_6(k_{10}k_{11})P + \\ &k_2k_8(k_4+k_5)(k_{10}+k_{11})Q + k_6k_8(k_2+k_4)(k_{10}+k_{11})QP + \\ &k_8k_{12}(k_4+k_5)(k_2+k_{10})QS + k_3k_5k_7(k_{10}+k_{11})B + k_3k_5k_8k_{11}BQ + \\ &k_3k_8k_{12}(k_5+k_{10})BQS + k_3k_6k_8(k_{10}+k_{11})BPQ + \\ &k_1k_7(k_4+k_5)(k_{10}+k_{11})A + k_1k_4k_6(k_{10}+k_{11})AP + \\ &k_1k_{10}k_{12}(k_4+k_5)AS + k_1k_3(k_5+k_7)(k_{10}+k_{11})AB + \\ &k_1k_3k_6(k_{10}+k_{11})ABP + k_1k_3k_{12}(k_5+k_{10})ABS\end{aligned} \quad (4)$$

Although the enzyme followed a strict compulsory ordered mechanism with acetaldehyde and

Abbreviations used: Adh, alcohol dehydrogenase (EC 1.1.1.1); Adh^S, slow alleloenzyme from *Drosophila melanogaster*; CIS, competitive inhibitor with stimulation; E, enzyme; A, NAD^+; Q, NADH; D, alcohol; B and S, aldehydes; P, carboxylate; I, inhibitor.

[1] To whom correspondence should be addressed.

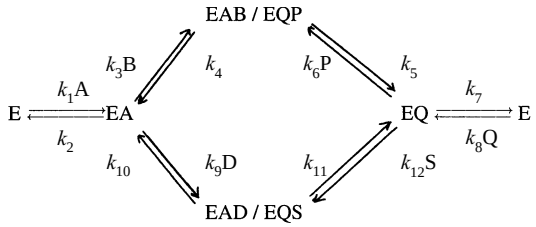

Scheme 1 An ordered reversible reaction pathway with altered inner substrates and products

Cleland [34,35] has previously described this reaction scheme for studies of alternative products. The rate expression for the liberation of Q with A, B, P, Q and S present is shown in eqn. (4), which was derived by the method of Fromm [36]. In the dismutation reaction of Adhs, A is NAD^+, Q is NADH, B and S represent aldehyde in the oxidation and reduction pathway respectively, D is ethanol and P is carboxylic acid. Table 1 describes the Dalziel kinetic coefficients (ϕ) for the forward and reverse reactions of both upper and lower pathways, the dismutation reaction and the corresponding coefficients for the product inhibition patterns for reversible reactions. To simplify the comparison of alternative product inhibition and dismutation reactions, the latter, and hence also the upper pathway, has been treated as a reversible reaction in the analysis.

acetone showed that these two compounds also formed binary complexes with the enzyme, which affected the binding of NAD^+ in the first phase of the reaction [16]. However, these studies did not answer whether the two binary enzyme complexes were involved in the oxidation of aldehydes to acids (eqn. 2) or in the NAD^+-plus-acetone induced isoenzyme conversion of Adh-5 into Adh-1 [17].

Previous metabolic studies have shown that Adh is the main enzyme in the oxidation of ethanol to acetic acid in *Drosophila* [18]. With both horse liver Adh and *Drosophila* Adh, acetaldehyde in the presence of NAD^+ underwent a dismutation reaction (eqn. 3), and at pH 7 equal amounts of acetate and ethanol were produced and hence no NADH could be detected [8,19,20]. This was due to the combined effect of the reactions described in eqns. (1) and (2); Scheme 1 shows the dismutation reaction for a strict compulsory ordered pathway. However, above pH 9 it has been possible to detect NADH production with *Drosophila* Adh [5,7,8] where an unequal amount of ethanol and acetate is produced in the dismutation reaction. Henehan et al. [8] have emphasized that the increase in A_{340}, i.e. the release of NADH, is not a direct measure of the aldehyde oxidation reaction and acetate production, and that the resulting kinetic values cannot be compared with those for alcohol dehydrogenation. Based on this, it should be assumed that the aldehyde oxidation reaction can only be determined by methods such as ^{1}H-NMR, gas chromatography or pH-stat titrations.

In studying the oxidation of aldehydes with methods such as ^{1}H-NMR or gas chromatography, initial-rate measurements are not possible, and these detection methods suffer the limitation that a large amount of enzyme is required to produce suitable amounts of product. The value of results obtained from initial-rate studies based on the increase in A_{340} has been questioned with respect to the type of information obtained. Therefore, we have analysed the kinetic coefficients obtained and compared them with those resulting for a simple aldehyde dehydrogenase reaction. The study shows that the kinetic coefficients determined from the increase in A_{340} at high pH during the oxidation/dismutation of aldehydes can be used, not only to determine the liberated NADH, but also to determine the amount of acetate formed under initial-rate conditions. Furthermore, it is possible to study the substrate specificity and to compare it with that of alcohol dehydrogenation. Dead-end and product inhibitors can be regarded mainly as in the case of a simple aldehyde dehydrogenase reaction and can be used to determine the reaction mechanism as well as the kinetic coefficients included in the dismutation reaction terms ϕ_{0d} and ϕ_{Ad} respectively. Consequently, the oxidation of aldehydes by *Drosophila* Adh has been studied through the increase in A_{340}, which due to the fluorimetric method used, required only nanomolar concentrations of the enzyme. The use of different aldehydes, product and dead-end inhibitors resulted in the determination of kinetic coefficients, the amount of acetate and NADH produced, the substrate specificity and the reaction mechanism.

EXPERIMENTAL

Reagents

Grade III NAD^+, NADH, Cibacrone Blue 3G-A and 1-[$^2H_1$]-acetaldehyde were from Sigma. Ethanol (96 %) was obtained from A/S Vinmonopolet. Anhydrous acetaldehyde (puriss p.a.), 2-chloroacetaldehyde, trimethylacetaldehyde (2,2-dimethylpropanal), imidazole, pyrazole and dioxan were from Fluka. Potassium acetate and propan-2-ol (99.7 %) were purchased from Merck.

Enzyme

D. melanogaster Adh^S was purified as described previously [21]. Freeze-dried samples were dissolved in 0.1 μM phosphate buffer, pH 7.0, and dialysed against two changes of the same buffer at 4 °C. Denaturated protein was removed by centrifugation for 20 min at 25000 ***g***.

Rate assay

To determine the amount of enzyme, i.e. the enzyme active-site concentration in the assay cuvette, the previously described spectrophotometric rate assay for *Drosophila* Adh was used [22]. The enzyme concentration is expressed as the amount of subunits in nanomoles. This is twice the amount of enzyme molecules, as the enzyme is a dimer. The assay solution consisted of 0.5 mM NAD^+ and 100 mM ethanol in a total volume of 1 ml of 0.1 M glycine/NaOH buffer, pH 9.5.

Kinetic measurements

The oxidation of aldehydes was studied by steady-state kinetics, and the inital rates were measured by following the appearance of NADH fluorescence using a sensitive filter fluorimeter based on the design previously described by Theorell and co-workers [23,24]. The light source was a mercury lamp (Osram Wotan Hg/2) enclosed in a water-cooled jacket. To obtain optimum stability, the lamp was supplied with power from a constant-voltage transformer with a current of 1.1–1.2 A. The exciting light is condensed by a glass lens through a Zeiss M366 filter with a transmission maximum at 366 nm and zero transmission above 400 nm and below 340 nm. The fluorescent light passes through the combination of a Jena FG10 filter, which absorbs scattered light, and a Jena GG420 filter, which results in the absorption of all light below 417 nm and gives 60 % transmission at 460 nm. Exciting light and fluorescent light pass through slits which can be varied in width from 1 mm to 8 mm in 1 mm increments. The cell compartment is a cylindrical water thermostated block which has four positions for $1 \times 1 \times 4.5$ cm cuvettes. The detector is an EMI 9656A photomultiplier with voltage supplied by a Keithly 246 EHT power pack and stabilized by a xenon dynode (154150) across the first stage. The current from the photomultiplier is measured by a Keithly 414S picoammeter which incorporates variable amplification and variable potential, enabling high

Table 1 Kinetic coefficients describing the initial rate for the forward and backward reactions, product and alternative product inhibition for the upper pathway, lower pathway and the dismutation reaction shown in Scheme 1

The general initial-rate equation (eqn. 4) is rearranged and described in the form of Dalziel coefficients [30], where unprimed coefficients describes the forward reactions and primed coefficients the backward reactions. The general rate equation is only shown for the forward reaction of the upper pathway, eqn (5), for S as an alternative product inhibitor of this pathway, eqn. (6), and for the dismutation reaction, eqn. (7). The rate equation for the lower pathway, the reverse pathways, other product or alternative product as inhibitors will be similar to these equations. Notice that the rate equation for the dismutase reaction (eqn. 7) is identical with the rate equation (eqn. 6), i.e. with S as an alternative product inhibitor of the upper forward pathway, as S equals B in the dismutation reaction. However, the dismutation reaction with aldehydes is an irreversible reaction, i.e. the upper pathway, and hence the oxidation of an aldehyde, is an irreversible process. Therefore P will not act as a product inhibitor in the dismutation reaction. For curiosity, we show the kinetic coefficients for P as a product inhibitor of both a reversible upper pathway and a reversible dismutation reaction.

Upper pathway

$\phi_{0u} = (k_5 + k_7)/k_5k_7 \quad \phi_A = 1/k_1 \quad \phi_B = (k_4 + k_5)/k_3k_5 \quad \phi_{AB} = k_2(k_4 + k_5)/k_1k_3k_5$

$\phi'_{0u} = (k_2 + k_4)/k_2k_4 \quad \phi_Q = 1/k_8 \quad \phi_P = (k_4 + k_5)/k_4k_6 \quad \phi_{PQ} = k_7(k_4 + k_5)/k_8k_4k_6$

Rate equation for the forward reaction:

$e/v = \phi_{0u} + \phi_A/[A] + \phi_B/[B] + \phi_{AB}/[A][B]$ (5)

Product inhibition

P: $K_{ip} = (k_5 + k_7)/k_6 \quad \phi_{PQ}/\phi_Q = k_7(k_4 + k_5)/k_4k_6$ Q: $K_{iq} = \phi_{PQ}/\phi_P = k_7/k_8$

B: $K_{ib} = (k_2 + k_4)/k_3 \quad \phi_{AB}/\phi_A = k_2(k_4 + k_5)/k_3k_5$ A: $K_{ia} = \phi_{AB}/\phi_B = k_2/k_1$

S as alternate product inhibitor

$K_{aiS} = (k_5 + k_7)(k_{10} + k_{11})/k_{12}(k_5 + k_{10}) \quad \phi_{SQ}/\phi_Q = k_7(k_{10} + k_{11})/k_{10}k_{12}$

Rate equation for the forward reaction with S as alternate product inhibitor:

$e/v = \phi_{0u}\,(1 + [S]/K_{aiS}) + \phi_A/[A] + (\phi_B + \phi_{AB}/[A])\{1 + [S]/(\phi_{SQ}/\phi_Q)\}/[B]$ (6)

Lower pathway

$\phi_{0l} = (k_7 + k_{11})/k_7k_{11} \quad \phi_A = 1/k_1 \quad \phi_D = (k_{10} + k_{11})/k_9k_{11} \quad \phi_{AD} = k_2(k_{10} + k_{11})/k_1k_9k_{11}$

$\phi'_{0l} = (k_2 + k_{10})/k_2k_{10} \quad \phi_Q = 1/k_8 \quad \phi_S = (k_{10} + k_{11})/k_{10}k_{12} \quad \phi_{SQ} = k_7\,(k_{10} + k_{11})/k_8k_{10}k_{12}$

Product inhibition

S: $K_{iS} = (k_7 + k_{11})/k_{12} \quad \phi_{SQ}/\phi_Q = k_7(k_{10} + k_{11})/k_{10}k_{12}$ Q: $K_{iq} = \phi_{PQ}/\phi_P = k_7/k_8$

D: $K_{id} = (k_2 + k_{10})/k_9 \quad \phi_{AD}/\phi_A = k_2(k_{10} + k_{11})/k_9k_{11}$ R: $K_{ia} = \phi_{AD}/\phi_D = k_2/k_1$

P as alternate product inhibitor

$K_{aip} = (k_4 + k_5)(k_7 + k_{11})/k_6(k_4 + k_{11}) \quad \phi_{PQ}/\phi_Q = k_7(k_4 + k_5)/k_4k_6$

Dismutation reaction (upper pathway and S = B)

$\phi_{0d} = \phi_{0u} + \phi_B\phi_Q/\phi_{SQ} + \phi_{0u}[B]/K_{aiS} = \{k_1k_3(k_5 + k_7)(k_{10} + k_{11}) + k_1k_{10}k_{12}(k_4 + k_5) + k_1k_3k_{12}(k_5 + k_{10})[B]\}/k_1k_3k_5k_7(k_{10} + k_{11})$

$\phi_{Ad} = \phi_A + \phi_{AB}\phi_Q/\phi_{SQ} = [k_3k_5k_7(k_{10} + k_{11}) + k_2k_{10}k_{12}(k_4 + k_5)]/k_1k_3k_5k_7(k_{10} + k_{11})$

$\phi_{Bd} = \phi_B \quad \phi_{ABd} = \phi_{AB}$

Rate equation:

$e/v = \phi_{0u}(1 + [B]/K_{aiS}) + \phi_B\phi_Q/\phi_{SQ} + (\phi_A + \phi_{AB}\phi_Q/\phi_{SQ})/[A] + \phi_B/[B] + \phi_{AB}/[A][B]$

or

$e/v = \phi_{0d} + \phi_{Ad}/[A] + \phi_{Bd}/[B] + \phi_{ABd}/[A][B]$ (7)

Product inhibition

P: $K_{ipd} = K_{ip}\phi_{0d}/\phi_{0u} \quad \phi_{PQ}/\phi_Q = k_7(k_4 + k_5)/k_4k_6$

Q: $K_{iqd} = f_1K_{iq} \quad f_1 = (\phi_{Ad}[B] + \phi_{AB})/(f_2\phi_{Ad}[B] + \phi_{AB})$

fluorescence signals to be backed off. The latter is an essential condition for the accurate measurement of slow initial rates when high sensitivity is used. A Keithly 370 chart-recorder was used.

The present study of aldehyde oxidation was performed with various concentrations of either aldehyde or NAD^+ in 0.1 M pyrophosphate buffer, pH 9.5, at 23.5 °C in the presence or absence of product and dead-end inhibitors. To normalize the results due to day-to-day variations in the light intensity of the xenon lamp, the deflection of a fluorescent Perspex standard (equivalent to an NADH concentration of about 7 μM) was measured at intervals during initial-rate measurements. Since NADH fluorescence is quenched by increasing NADH concentrations, calibration curves of the fluorescence of NADH against NADH concentration were determined for different slit-width combinations. In the present study, slit widths of 2 mm for both exciting and emitted light were used. The standard curve was linear for between 10^{-8} M and 3×10^{-5} M NADH. All initial-rate determinations were within the linear part of the standard curve. In all the experiments, the reported aldehyde concentrations represent the sum of the free and hydrated species present.

Inhibition of the alcohol oxidation and the aldehyde reduction pathway was studied at a constant concentration of either alcohol or aldehyde while varying coenzyme concentration, and at a constant concentration of coenzyme while varying alcohol or acetaldehyde concentration. These studies were performed either with the filter fluorimeter or spectrophotometrically at 340 nm, in 0.1 M pyrophosphate buffer, pH 9.5, at 23.5 °C. A Perkin-Elmer Lambda 15 spectrophotometer coupled to a computer was used along with the Perkin-Elmer program PECSS.

RESULTS

Problems that need attention in the study of aldehyde reactions are the choice of buffer and the fact that some aldehydes can react with the nicotinamide moiety of NAD^+ at basic pH. Recently, Henehan et al. [8] studied the problem of buffer choice in aldehyde oxidation reactions. They showed that nitrogen-containing buffers react with aldehyde to produce Schiff bases, which then gave rise to polymerization reactions. In the present work, a mixture of acetaldehyde and NAD^+ in 0.1 M glycine/NaOH buffer (pH 9.5 and 23.5 °C) resulted in large time-dependent fluorescence increments, probably due to the pro-

Table 2 Kinetic parameters for the oxidation of aldehydes to acids with the *D. melanogaster* Adh^S at pH 9.5 and 23.5 °C

Experiments were performed as described in the Materials and methods section. The concentration range of the different aldehydes was as follows: acetaldehyde, 1–30 mM; 1-[$^2H_1$]acetaldehyde, 0.5–30 mM; trimethylacetaldehyde, 0.5–10 mM. The different kinetic coefficients were derived from non-linear regression using the ENZFITTER program (Elsevier-BIOSOFT). No corrections have been made for the differences in *gem*-diol content.

Substrate	*Gem*-diol (%)	k_{cat} (s^{-1})	K_m (mM)	k_{cat}/K_m ($s^{-1}M^{-1}$)
Acetaldehyde	57	0.25 ± 0.01	1.7 ± 0.2	145.6
1-[$^2H_1$]acetaldehyde	57	0.29 ± 0.01	6.8 ± 0.8	42.6
Trimethylacetaldehyde	19	0.21 ± 0.01	2.4 ± 0.2	87.5

duction of NADH-like adducts and Schiff bases [25,26]. This problem was avoided by using 0.1 M pyrophosphate buffer (pH 9.5), where no background activity appeared with either acetaldehyde or trimethylacetaldehyde. Owing to the hydrophobic nature of trimethylacetaldehyde, it was necessary to dissolve it in 50% dioxan, and in the reaction assays a total concentration of 1% dioxan resulted. Previously we have shown that this dioxan concentration has no effect on the oxidation of alcohols [27]. It is noteworthy that 2-chloroacetaldehyde (97% *gem*-diol), on reaction with NAD^+, produced an extreme background reactivity in both glycine and pyrophosphate buffers. This prevented the use of this aldehyde in the present study of aldehyde oxidation.

Substrate specificity

As mentioned previously, it was possible to measure the production of NADH at pH 9.5 [5,7,8]. However, due to the dismutation reaction (eqn. 3 and Scheme 1) a filter fluorimeter with high sensitivity was necessary to obtain reliable initial-rate measurements. Although the initial-rate curve was always linear over a measurable range, it was noticeable that the deviation from linearity occurred sooner with increasing aldehyde concentrations or decreasing NAD^+ concentrations. This prevented us from varying both the aldehyde and NAD^+ concentrations, and hence achieving a direct determination of the four different Dalziel coefficients, i.e. the ϕ values (Table 1). Therefore only the

Table 3 Inhibition constants derived from product, alternate product and dead-end inhibition studies with the *D. melanogaster* Adh^S

[a]Concentration of fixed substrate in paranthesis. [b]C = competitive, NC = non-competitive, UC = uncompetitive, CIS = competitive inhibition with stimulation, ps = re-plot of slopes is parabolic. [c]The inhibition constants were derived from slopes $K_{is} = [I]/[(s_i/s_0)-1]$ or from intercepts $K_{ii} = [I]/[(Int_i/Int_0)-1]$ unless stated otherwise, where the subscripts i and 0 denote with or without inhibitor respectively. [d]The results are presented as mean values with an average S.D. of less than 10% of the mean. [e]From Winberg et al. [27]. [f]The inhibitory constant is derived from the intercept effects with $K_{EA,I} = K_{ii}/\{(\phi_0[D]/\phi_D)+1\}$ where $\phi_0 = 0.74$ s and $\phi_D = 2.5$ mM s. [g]No constants determined due to the non-linear re-plots. [h]From Hovi*k* et al. [28]. [i]$K_{E,I} = K_{is}/\{(\phi_D[A]/\phi_{AD})+1\}$, where K_{is} is derived as in [c], $\phi_D = 2.5$ mM s and $\phi_{AD} = 0.029$ mM^2 s. [j]$K_{E,I} = K_{ii}/((\phi_0[A]/\phi_A)+1)$, where K_{ii} is derived as in [c], $\phi_0 = 0.74$ s and $\phi_A = 6.0$ μM s. [k]The kinetic coefficients derived from these constants in the case of product or alternative product inhibition are described in Table 1. [l]From Winberg and McKinley-McKee [16]. ϕ_0, ϕ_A, ϕ_D and ϕ_{AD} are from Winberg and McKinley-McKee [14].

Inhibitor	Varied substrate	Fixed substrate[a] (mM)	Type of inhibition[b]	Inhibition constant[c]	Value[d]
Pyrazole	Ethanol	NAD^+ (0.5)	C	$K_{is} = K_{EA,I}$ (μM)	4.4[e]
	NAD^+	Ethanol (100)	UC	$K_{EA,I}$ (μM)	5.3[f]
	Acetaldehyde	NAD^+ (0.5)	NC	K_{is} (μM)	3.3
				K_{ii} (μM)	5.1
	NAD^+	Acetaldehyde (6.0)	NC	K_{is} (μM)	2.3
				K_{ii} (μM)	4.8
	Trimethylacetaldehyde	NAD^+ (0.5)	NC	K_{is} (μM)	2.6
				K_{ii} (μM)	7.6
	NAD^+	Trimethylacetaldehyde (mM)	NC	K_{is} (μM)	4.5
				K_{ii} (μM)	3.2
Imidazole	Propan-2-ol	NAD^+ (0.5)	CIS	K_{is} (M)	1.3
	NAD^+	Propan-2-ol (0.5)	CIS(ps)	—[g]	–
	Acetaldehyde	NAD^+ (0.5)	CIS(ps)	—[g]	–
	NAD^+	Acetaldehyde (6.0)	CIS(ps)	—[g]	–
Cibacrone Blue	NAD^+	Ethanol (500)	C	$K_{is} = K_{E,I}$ (μM)	8.0[e]
	NAD^+	Butan-2-ol (7.5)	C	$K_{is} = K_{E,I}$ (μM)	3.0[h]
	Ethanol	NAD^+ (0.5)	NC	$K_{E,I}$ from K_{is} (μM)	2.4[e,i]
				$K_{E,I}$ from K_{ii} (μM)	2.5[e,j]
	NAD^+	Acetaldehyde (6.0)	C	K_{is} (μM)	2.1
	NAD^+	Acetaldehyde (0.67)	C	K_{is} (μM)	2.0
	Acetaldehyde	NAD^+ (0.1)	NC	K_{is} (μM)	14.9
				K_{ii} (μM)	18.1
Acetate	Ethanol	NAD^+ (0.5)	NC	K_{is} (mM)	66[k]
				K_{ii} (mM)	912[k]
	NAD^+	Ethanol (500)	UC	K_{ii} (mM)	319[k]
	NAD^+	Ethanol (2.5)	UC	K_{ii} (mM)	83[k]
	Acetaldehyde	NAD^+ (0.5)	NC	K_{is} (mM)	70[k]
				K_{ii} (mM)	143[k]
	NAD^+	Acetaldehyde (6.0)	NC	K_{is} (mM)	145[k]
				K_{ii} (mM)	124[k]
NADH	NAD^+	Ethanol (500)	C	$K_{is} = K_{iq}$ (μM)	3.8[k,l]
	NAD^+	Ethanol (5.7)	C	$K_{is} = K_{iq}$ (μM)	3.7[k,l]
	NAD^+	Propan-2-ol (5.0)	C	$K_{is} = K_{iq}$ (μM)	3.7[k,l]
	NAD^+	Acetaldehyde (6.0)	C	$K_{is} = K_{iqd}$ (μM)	0.11[k]

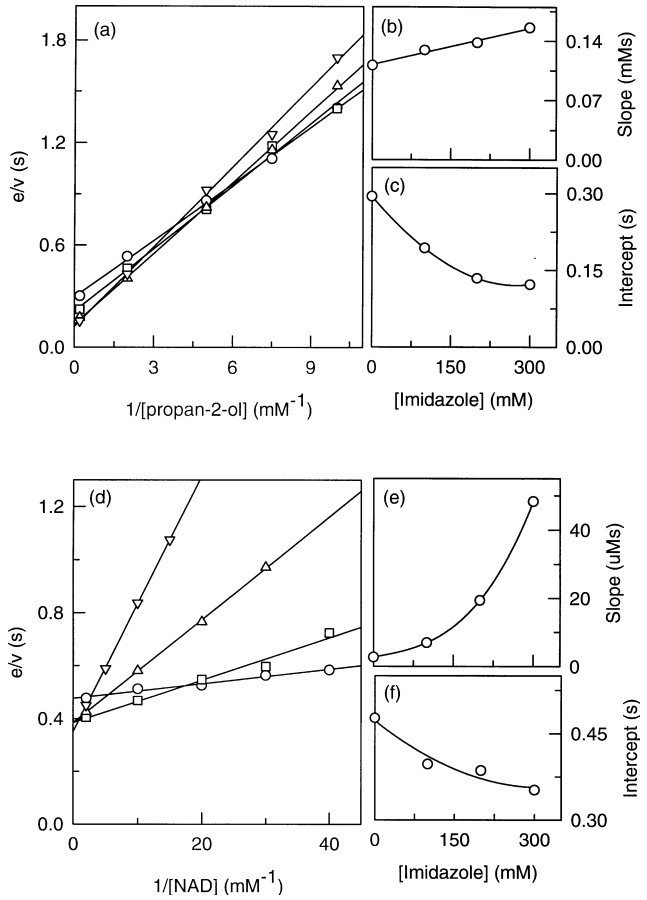

Figure 1 Imidazole as an inhibitor against propan-2-ol and NAD$^+$

[Imidazole]: ○, control; □, 100 mM; △, 200 mM; ▽, 300 mM. Primary plots with (**a**) varied propan-2-ol and a fixed NAD$^+$ concentration of 0.5 mM and (**d**) varied NAD$^+$ and a fixed propan-2-ol concentration of 0.5 mM. Re-plots of slopes (**b**,**e**) and intercepts (**c**,**f**) from (**a**) and (**d**) respectively versus imidazole concentration.

kinetic constants $k_{cat(app)}$, K_m and $k_{cat(app)}/K_m$ were determined for the different aldehydes using a constant saturating concentration of coenzyme. A constant concentration of 0.5 mM NAD$^+$ has been used in the experiments with varied aldehyde concentrations. Although the linear range of the inital-rate curve was increased with coenzyme concentrations of 1–2 mM, this advantage was counterbalanced by an increased background noise. It is also significant that at a given aldehyde concentration (including the highest and the lowest), the same initial velocity was obtained at 0.5 and 2 mM coenzyme. Thus the kinetic constants $k_{cat(app)}$ and $k_{cat(app)}/K_m$ obtained for the different aldehydes can be regarded as $1/\phi_{0d}$ or k_{cat} and $1/\phi_{Bd}$ or k_{cat}/K_m respectively (Table 1).

Oxidation of the different aldehydes followed a hyperbolic saturation curve (v versus A, where A is NAD$^+$) and gave a linear double-reciprocal plot (results not shown). Substrate inhibition was observed at acetaldehyde concentrations larger than 30 mM. The kinetic constants obtained are presented in Table 2. The three aldehydes investigated showed almost identical k_{cat} values. This shows that the optimal NADH release in the dismutation reaction at pH 9.5 is not dependent on the hydration level of the aldehyde or the presence of a heavy atom in the hydride-transfer reaction.

Even at the highest sensitivity of the fluorimeter, no activity could be detected with 100 mM acetate and 10 μM NADH at pH 9.5. This was also the case for the oxidation of acetaldehyde at pH 7.0. The lack of a time-dependent production of NADH fluorescence at neutral pH was previously shown to be due to the immediate use of the NADH produced in the dismutation reaction [8].

Product, alternate product and dead-end inhibition studies

Pyrazole

We have shown previously that pyrazole is an alcohol-competitive inhibitor which formed a strong ternary EAI complex, with a $K_{EA,I}$ value of 4.4 μM at pH 9.5 [14,27], where E is enzyme, A is NAD$^+$ and I is inhibitor. In the present work pyrazole has been tested to see if it could form a binary EI and/or a ternary EQI complex, where Q is NADH. Pyrazole was an uncompetitive inhibitor with either varied NAD$^+$ and a constant concentration of 100 mM ethanol at pH 9.5, or varied acetaldehyde and a constant NADH concentration at either pH 9.5 or 7.0. These results rule out the formation of EI and EQI complexes. As the intercept with pyrazole against varied NAD$^+$ was due to $\phi_0+\phi_D(1+[I]/K_{EA,I})/[D]$, where D is the alcohol, the inhibition constant was calculated by using the previously determined ϕ values [14] and the constant is listed in Table 3.

In the oxidation of aldehydes, pyrazole showed linear non-competitive inhibition with both varied aldehyde and a fixed NAD$^+$ concentration, and varied NAD$^+$ with a fixed concentration of either acetaldehyde or trimethylacetaldehyde. The inhibition constants that resulted from the slope and intercept effects are summarized in Table 3.

Imidazole

With either varied propan-2-ol and a fixed concentration of NAD$^+$, or varied NAD$^+$ and a fixed concentration of propan-2-ol, imidazole acted as a competitive inhibitor with stimulation (CIS) (Figures 1a and 1d). A linear re-plot of slopes from Figure 1(a) against imidazole concentration is shown in Figure 1(b) and the K_{is} value is presented in Table 3. A re-plot of intercepts against imidazole concentration (Figure 1c) showed that the intercept decreased with increasing imidazole concentration and the curve appears to be hyperbolic, with k_{cat} increasing approximately 2.5-fold in the presence of 300 mM of imidazole. It was not possible to increase the imidazole concentration further due to the resulting increase in background noise. Re-plots of the slopes from Figure 1(d) against the imidazole concentrations resulted in parabolic plots (Figure 1e). A re-plot of intercepts against imidazole also showed activation which appeared to be hyperbolic (Figure 1f). Owing to the low propan-2-ol concentration (0.5 mM), k_{cat} increased only 1.3-fold in the presence of 300 mM imidazole.

With 0.5 mM NAD$^+$ and ethanol concentrations of either 100 mM or 1.7 mM, the presence of 0, 100, 200 and 300 mM imidazole gave the following activities [v/e (s^{-1})]: 1.34, 1.66, 1.78, 1.68 and 0.42, 0.42, 0.43, 0.39 respectively. Thus with Adh^S, imidazole also acts as a CIS against ethanol. This shows that the dissociation of NADH from the binary EQ product complex is partly rate-limiting, along with the hydride-transfer step [28].

With either varied acetaldehyde and a fixed concentration of NAD$^+$ or varied NAD$^+$ and a fixed concentration of acetaldehyde, imidazole again acted as a CIS (Figures 2a and 2d). A re-plot of slopes from Figure 2(a) against imidazole concentration resulted in a parabolic plot (Figure 2b). A re-plot of intercepts against imidazole concentration showed that the intercept decreased with increasing imidazole concentration, and the curve appears to be hyperbolic (Figure 2c). As shown in Figure 2(c),

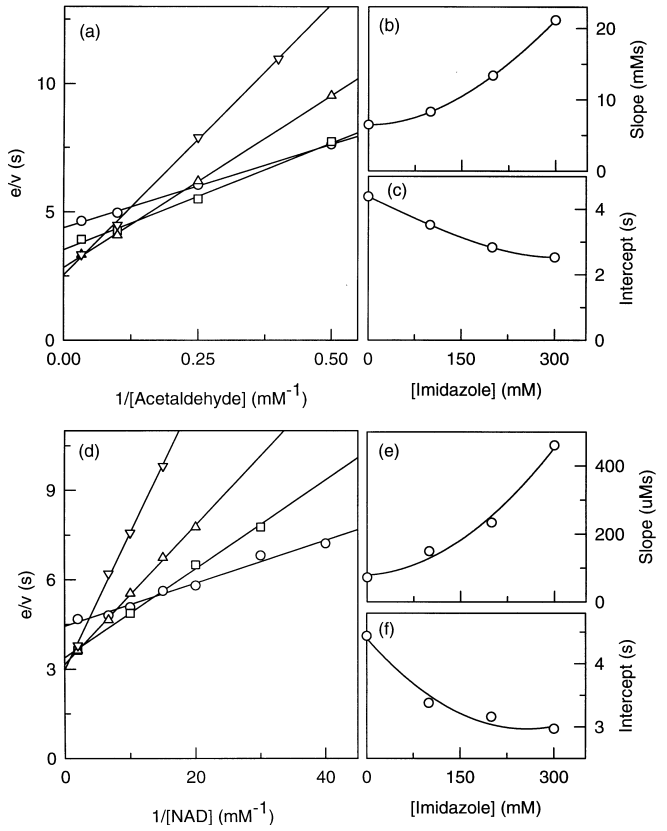

Figure 2 Imidazole as an inhibitor against acetaldehyde and NAD$^+$

[Imidazole]: ○, control; □, 100 mM; △, 200 mM; ▽, 300 mM. Primary plots with (**a**) varied acetaldehyde and a fixed NAD$^+$ concentration of 0.5 mM and (**d**) varied NAD$^+$ and a fixed acetaldehyde concentration of 6.0 mM. Re-plots of slopes (**b**,**e**) and intercepts (**c**,**f**) from (**a**) and (**d**) respectively versus imidazole concentration.

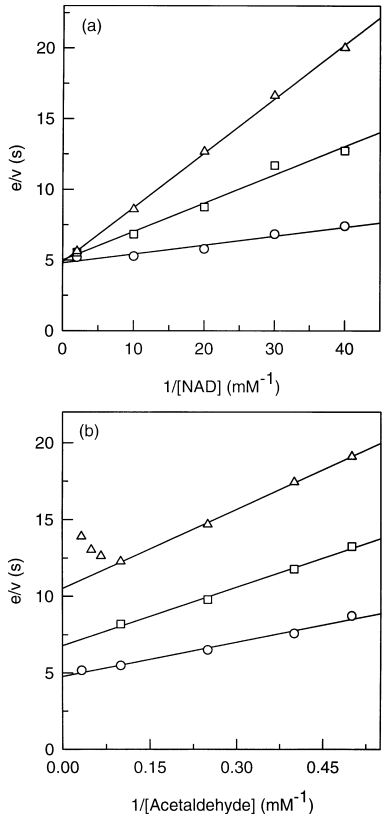

Figure 3 Cibacrone Blue 3GA as an inhibitor against NAD$^+$ and acetaldehyde

(**a**) Plot with varied NAD$^+$ and a fixed acetaldehyde concentration of 6.0 mM. [Cibacrone Blue]: ○, control; □, 5.0 μM; △, 10.0 μM. (**b**) Plot with varied acetaldehyde and a fixed NAD$^+$ concentration of 0.1 mM. [Cibacrone Blue]: ○, control; □, 10.0 μM; △, 20.0 μM.

k_{cat} increased approximately 1.7-fold in the presence of 300 mM imidazole. Re-plots of the slopes from Figure 2(d) against imidazole concentration also resulted in parabolic plots (Figure 2e). A re-plot of intercepts against imidazole also showed activation which appeared to be hyperbolic (Figure 2f), and k_{cat} increased 1.5-fold in the presence of 300 mM imidazole.

Cibacrone Blue 3 GA

Cibacrone Blue 3 GA is known to be a coenzyme-competitive inhibitor of *Drosophila* Adhs [27–29]. As shown in Figure 3(a), this is also the case in the aldehyde oxidation reaction when NAD$^+$ is varied and acetaldehyde is the fixed substrate. The K_{is} values obtained with fixed acetaldehyde concentrations of 6.0 and 0.67 mM are shown in Table 3. With varied acetaldehyde and a fixed NAD$^+$ concentration, non-competitive inhibition was observed (Figure 3b). In the presence of the inhibitor and high concentrations of acetaldehyde, the curve deviates from linearity and gives an upward curvature. This curvature is more pronounced at the higher inhibitor concentration.

Acetate

Non-competitive inhibition with varied ethanol and a fixed concentration of NAD$^+$ was obtained with acetate. Linear re-plots of slopes and intercepts resulted, and the inhibitor constants obtained are summarized in Table 3. Acetate was an uncompetitive inhibitor with varied NAD$^+$ and a fixed high (100 mM) or low (2.5 mM) concentration of ethanol. The K_{ii} values obtained are presented in Table 3.

Acetate was also a non-competitive inhibitor with both varied acetaldehyde and a fixed concentration of NAD$^+$, and varied NAD$^+$ and a fixed acetaldehyde concentration. Linear re-plots of slopes or intercepts against varied acetate concentrations resulted, with inhibitor constants as summarized in Table 3.

NADH

This compound was a competitive inhibitor with varied NAD$^+$ in the presence of a fixed acetaldehyde concentration. The re-plot of slopes against NADH concentrations was linear and the K_{is} obtained is listed in Table 3.

DISCUSSION

Analysis of the kinetic coefficients determined through NADH release in a dismutation reaction

Previous investigations with *Drosophila* Adh have shown that the oxidation of aldehydes to carboxylate at basic pH is accompanied by the liberation of NADH [5,7,8]. However, the production of detectable NADH was peripheral to the overall flux of acetaldehyde through dismutation, and the acetate and ethanol production continued after the disappearance of a net production

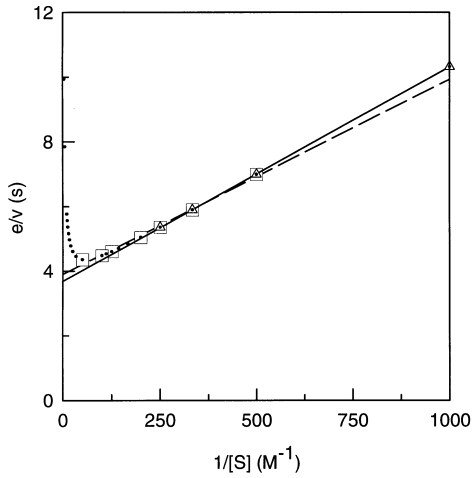

Figure 4 Theoretical curve based on eqn. (7) (Table 1), assuming an infinite concentration of A, which gives $e/v = \phi_{0u}(1+[B]/K_{aiS})+\phi_B\phi_Q/\phi_{SQ}+\phi_B/[B]$

In this example, $\phi_{0u} = 0.2$ s, $K_{aiS} = 9.5$ mM, $\phi_B\phi_Q/\phi_{SQ} = 3.4$ s and $\phi_B = 6.7$ mM and the small closed circles show the rate values obtained. With $[B]/K_{aiS} \ll$ M unity, ϕ_{0d} is 3.6. Linear regression on the four lowest points (△) gave an intercept of 3.69 s and a slope of 6.62 mM s, and on points which includes the inflection point (□) gave an intercept of 3.90 s and a slope of 6.03 mM s. In both cases, the estimated intercepts and slopes deviate less than 10% from the real ϕ_B value and the ϕ_{0d} value of 3.6 s.

of NADH, a phenomenon Henehan et al. [8] refer to as a steady-state burst effect. Therefore, they emphasized that the kinetic coefficients obtained through the determination of liberated NADH do not reflect the oxidation of an aldehyde to an acid, as would have been the case for a simple aldehyde dehydrogenase reaction. However, this is not entirely true, as shown in Scheme 1 and Table 1, where the relation between kinetic coefficients and rate constants for an ordered aldehyde oxidation, accompanied by a dismutation and a small NADH release, is described. In this analysis, the reaction rate is determined through the NADH release. In Scheme 1, aldehyde oxidation follows the upper pathway, and the aldehyde reduction giving rise to dismutation follows the lower pathway. This mechanism, which follows saturation kinetics at low aldehyde concentrations, is described by eqn. (4) and by eqn. (7) (Table 1). For dismutation, the double-inverse form in Dalziel nomenclature [30], shown in eqn. (7), is identical with the expression for S as an alternate product inhibitor of the upper pathway, eqn. (6) (Table 1), as S = B in the dismutation reaction.

It is noticeable that the two kinetic coefficients ϕ_{Bd} and ϕ_{ABd} are identical with the corresponding coefficients for the upper pathway alone (ϕ_B and ϕ_{AB}), and hence reflect the true coefficients for aldehyde oxidation, i.e. a simple aldehyde dehydrogenase reaction (Table 1). This shows that the substrate specificity with respect to aldehydes can be determined in a continuous initial-rate assay that determines the NADH release, and this can be treated and compared with the corresponding coefficients for alcohol oxidation. However, the other two kinetic coefficients, ϕ_{0d} and ϕ_{Ad}, are more complex and involve the dismutation reaction. Table 1 shows that ϕ_{0d} is made up of three terms, ϕ_{0u} which reflects the acid production at infinite substrate concentrations, $\phi_B\phi_Q/\phi_{SQ}$ and $\phi_{0u}[B]/K_{aiS}$. The last two terms include the conversion of aldehyde into alcohol through the lower pathway in Scheme 1. With varied aldehyde and a fixed NAD^+ concentration, the double-inverse curve will deviate from linearity at high aldehyde concentrations, and show substrate inhibition due to the term $\phi_{0u}[B]/K_{aiS}$. The term $\phi_B\phi_Q/\phi_{SQ}$ (Table 1) is derived from both the EA complex (ϕ_B) and the free enzyme (ϕ_Q/ϕ_{SQ}). The latter term reflects the binding of Q to the free enzyme E and the aldehyde flux through the lower pathway (Scheme 1 and Table 1). Therefore the $\phi_B\phi_Q/\phi_{SQ}$ term must be considered in studies with dead-end inhibitors, as an inhibitor that binds only to the EA form and is competitive with an alcohol will be non-competitive with an aldehyde in a dismutation reaction. As ϕ_{Ad} is determind by extrapolation to an infinite aldehyde concentration, this constant reflects the formation of EA in the system (Table 1).

In the present work it was necessary to study the reaction at a fixed high saturating concentration of NAD^+ in order to obtain reliable results. Figure 4 shows a theoretical curve based on eqn. (7), assuming an infinite NAD^+ concentration and the arbitrary kinetic coefficients described in the legend. As shown in the Figure, it is possible to include velocity data for substrate concentrations close to the inflection point in the extrapolation of the apparently linear parts of the curve, and the intercept and slope obtained will deviate by less than 10% of the theoretical values of ϕ_{0d} and ϕ_{Bd} respectively. This suggests that the experimentally obtained values of intercepts and slopes can be regarded, within the experimental error, as ϕ_{0d} and ϕ_{Bd}. ϕ_{0d} reflects the release of NADH under inital-rate conditions, but not the quantitative production of carboxylate. Hovewer, it is possible to estimate the carboxylate production (ϕ_{0u}) through dead-end inhibition studies, from which it is possible to determine the quantitative contribution of the different terms included in the ϕ_{0d} coefficient obtained.

Product and dead-end inhibitors can be used to determine the reaction mechanism of the aldehyde oxidation reaction. In principle, the results obtained can be interpreted essentially as for a simple aldehyde dehydrogenase reaction.

Reaction mechanism for the oxidation and dismutation of aldehydes with *Drosophila* Adh

Previous studies with different *Drosophila* Adhs showed that the lower pathway in Scheme 1, i.e. the oxidation of alcohols and reduction of aldehydes, followed a strict compulsory ordered reaction mechanism, with coenzymes as the outer substrates [3,16]. However, it is not known whether the oxidation of aldehydes follows a compulsory or a random ordered pathway, as product inhibition studies with acetaldehyde showed that a binary EB complex was formed [16]. Whether this was a dead-end complex or a part of the aldehyde oxidation mechanism was not shown.

The present work with the Adh^S shows that imidazole acts as a CIS with varied concentrations of propan-2-ol and fixed NAD^+ (Figure 1a) or varied NAD^+ and fixed propan-2-ol (Figure 1d). The stimulatory effect on the intercepts (Figures 1c and 1f) is due to the formation of a ternary EQI complex from which Q dissociates faster than from the EQ complex which is rate limiting. If an EQ complex is formed in the oxidation of aldehydes, imidazole and aldehyde should compete for binding to this complex. It should be noted that in the ordered dismutation reaction shown in Scheme 1, the formation of an EQI complex should result in stimulation, even if the rate-limiting step of the reaction were the interconversion of the ternary complexes or the release of P from the EQP complex, where P is the carboxylate ion. This distinguishes the dismutation reaction from the simple ordered oxidation of alcohols (lower pathway in Scheme 1), in which stimulation can be detected only if dissociation of Q from the EQ complex is at least partly rate-limiting. In a random

ordered mechanism with the formation of a binary EP complex, it should only be possible to detect the EQ complex if it is formed in such quantities that it significantly contributes to the reaction. In Figures 2a, 2c, 2d and 2f, it can be seen that imidazole acts as a CIS with both varied acetaldehyde and a fixed concentration of NAD^+ and with varied NAD^+ and a fixed acetaldehyde concentration. Stimulation of the intercept term, ϕ_{0d}, (Figures 2c and 2f) was quantitatively comparable with that of propan-2-ol oxidation (Figures 1c and 1f). The imidazole experiments demonstrate that under the initial-rate conditions used, a kinetically significant EQ complex is formed in the oxidation of acetaldehyde to acetate.

In order to determine whether or not acetate formed a binary EP complex, acetate was used as an alternative product inhibitor to varied NAD^+ with fixed high and low concentrations of ethanol. An uncompetitive inhibition was observed in both cases, which showed that acetate does not form a binary EP complex, and hence it can be concluded that the second phase of the aldehyde oxidation pathway (Scheme 1) follows an ordered mechanism where acetate (P) leaves the ternary EQP complex and forms an EQ complex.

Previously it was shown that Cibacrone Blue was a coenzyme competitive inhibitor of *Drosophila* Adhs, and Table 3 lists the dissociation constant ($K_{E,I}$) obtained for the Adh^S. Cibacrone Blue is also a competitive inhibitor with varied NAD^+ at a fixed acetaldehyde concentration (Figure 3a), and the inhibitor constant is independent of the fixed level of acetaldehyde or whether the fixed substrate is an alcohol (Table 3). Cibacrone Blue is a non-competitive inhibitor with varied acetaldehyde and a fixed NAD^+ concentration (Figure 3b). This was also the case with varied ethanol and a fixed NAD^+ concentration [27], and the $K_{E,I}$ values from these experiments have been calculated using the previously determined ϕ values for the Adh^S enzyme (Table 3). The most noticeable trait of Figure 3(b) is that the curve deviates from linearity at high acetaldehyde concentrations in the presence of the inhibitor. This is all consistent with a compulsory ordered reaction mechanism and the ordered mechanism for the dismutation reaction as shown in Scheme 1, where Cibacrone Blue binds to the free enzyme. At high acetaldehyde concentrations, aldehyde binds to the EI complex and forms an EIB complex, which causes the deviation from linearity in Figure 3(b). This indicates that the ϕ_{Ad} and the ϕ_{ABd} terms should be multiplied by $\{1+([I]/K_{E,I})(1+[B]/K_{EI,B})\}$ [31,32]. Therefore at acetaldehyde concentrations up to 6 mM, the $[B]/K_{EI,B}$ term must be much less than unity, but this term begins to contribute to the inhibition pattern at aldehyde concentrations above 10 mM. A rapid equilibrium random mechanism where the NAD^+ and the aldehyde subsites behave independently could give identical K_i values at different fixed acetaldehyde concentrations. In a steady-state random mechanism I can induce substrate inhibition by B if B slows down the release of I. However, neither of these two mechanisms alone can give rise to the inhibition pattern obtained with Cibacrone Blue. Therefore, the inhibition studies show that the oxidation of aldehydes is only consistent with a compulsory ordered mechanism as shown in Scheme 1. This also shows that the binary EB complex determined in the previous product inhibition study [16] was a dead-end complex.

Inhibitor complexes formed

The oxidation of aldehydes has been regarded as an irreversible process [8,19], and the present work supports this conclusion, as no enzymic activity was observed in the presence of acetate or NADH. Acetate was an uncompetitive inhibitor with NAD^+ at both high and low ethanol concentrations, which also supports this conclusion and in addition shows that acetate does not form a binary EP complex. With varied ethanol and a fixed NAD^+ concentration, acetate gave a non-competitive pattern. This pattern shows that acetate formed a ternary EAP complex (slope effects) and a ternary dead-end EQP complex in the second phase of the reaction (intercept effects). The inhibition constants are listed in Table 3. The K_{ii} value obtained from varied ethanol is larger than the true $K_{EQ,P}$ value, as the EQP complex only affects the term in ϕ_{0i} that is derived from the EQ complex. The K_{ii} values obtained from the effect on the intercept of varying the concentration of NAD^+ are consistent with the formation of both an EAP and EQP complex.

In the oxidation of acetaldehyde, acetate is a non-competitive inhibitor with respect to both acetaldehyde and NAD^+. The slope effect obtained with varied acetaldehyde is due to the formation of a ternary EAP complex, and the inhibition constant obtained is comparable with that obtained with ethanol as the varied substrate (Table 3). In the dismutation reaction of acetaldehyde, the large intercept effects are, in addition to the EQP complex, also due to the EAP complex, as ϕ_{0d} includes the term $\phi_B\phi_Q/\phi_{SQ}$ which should be multiplied by $(1+[P]/K_{EA,P})$ in the presence of acetate. It is noticeable that acetate is a non-competitive inhibitor of varied NAD^+ in the oxidation of acetaldehyde, as the studies with ethanol showed that acetate does not form a binary EP complex. With varied NAD^+ the slope is $\phi_{Ad}+\phi_{ABd}/[B]$, and in a compulsory ordered mechanism (including the dismutation reaction in Scheme 1) both coefficients are determined by the free enzyme E. As acetate does not form a binary EP complex, the slope effects imply the formation of a dead-end ternary EBP complex. In a compulsory ordered pathway (Scheme 1) with a dead-end EB complex, the formation of an EBP complex should only affect the ϕ_{Ad} term, which should be multiplied by $[1+\{([B]/K_1)+[\phi_{AB(d)}/\phi_{A(d)}\,K_1]\}(1+[I]/K_2)]$ (see [32]), where K_1 represents $K_{E,B}$ and K_2 represents $K_{EB,P}$.

The two heterocyclic $C_3N_2H_4$ compounds pyrazole and imidazole produced various complexes with the enzyme and its intermediates. Imidazole in contrast to pyrazole gave both EI and EQI complexes and Figures 1e and 2e suggest that two or more imidazole molecules bind to the free enzyme. Both inhibitors form a ternary EAI complex. The EAI complex with imidazole was weak and the $K_{EA,I}$ value was calculated to be 1.3 M (Table 3). Pyrazole formed a strong EAI complex, as seen from the effect on the slope (K_{is}), with either varied ethanol, acetaldehyde or trimethylacetaldehyde (Table 3). It is noticeable that pyrazole was a non-competitive inhibitor with varied NAD^+ in the oxidation of both acetaldehyde and trimethylacetaldehyde. As pyrazole, like acetate, did not form a a binary EI complex, it can be concluded that both acetaldehyde and trimethylacetaldehyde form a dead-end binary EB complex, and pyrazole can bind to both EB complexes and form with each a ternary EBI complex. As shown in Table 3, the binding of pyrazole to the two EB complexes gave similar K_{is} values. However, these are complex, as in the case of acetate, and involve the constants for the EB and EBI complexes. Scheme 2 summarizes the reaction mechanism for the oxidation of aldehydes, the corresponding dismutation reaction and the different inhibition complexes that are formed by Adh^S from *D. melanogaster*.

Estimation of the kinetic coefficients and their individual terms in the dismutation reaction

Based on the inhibition studies and the ordered reaction mechanism in Scheme 1, it is possible to estimate both the magnitude of the different ϕ values and also the values of the different individual terms that give rise to the ϕ_{0d} and ϕ_{Ad} coefficients. In

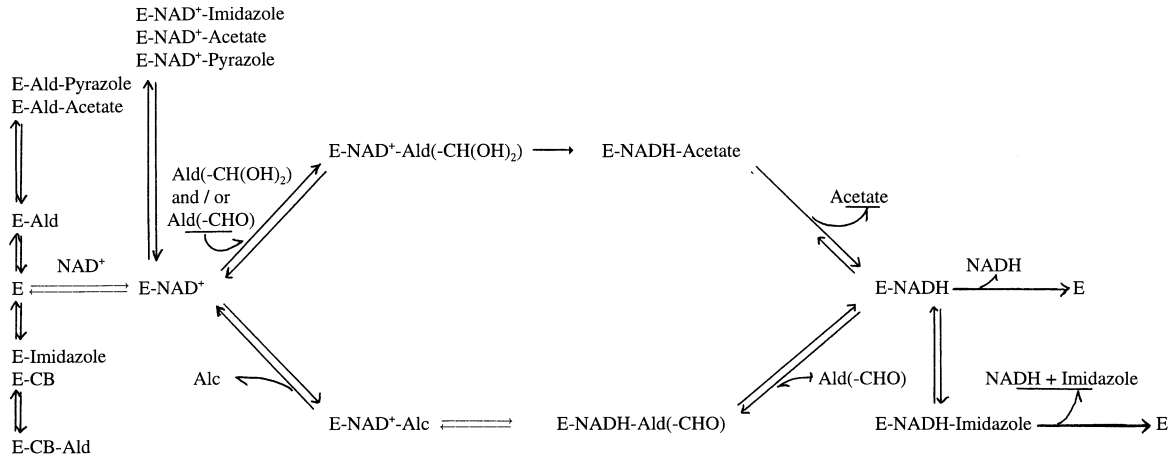

Scheme 2 Mechanism for the dismutation reaction of aldehydes and the different complexes formed between *D. melanogaster* Adh^S and dead-end inhibitors

E is enzyme, CB is Cibacrone Blue , Ald(-CHO) is the carbonyl form of acetaldehyde or trimethylacetaldehyde, Ald(-CH(OH)$_2$), is the *gem*-diol form of acetaldehyde or trimethylacetaldehyde, Ald indicates that it is not clear which form of the aldehyde is involved in binding and Alc is alcohol.

the experiments with varied acetaldehyde, a fixed concentration of either 0.5 or 0.1 mM NAD^+ was used. The slope is $\phi_{Bd}+\phi_{ABd}/[A]$, and ϕ_{ABd} can be written as $\phi_{Bd}K_{E,A}$. Previously $K_{E,A}$ was determined to be 16 μM [14] and based on the k_{cat}/K_m value in Table 2 (0.5 mM NAD^+) and the slope value of 7.5 mM s, obtained with a fixed NAD^+ concentration of 0.1 mM, ϕ_{Bd} is estimated to be 6.6 mM s and ϕ_{ABd} to be 0.106 mM^2 s.

The ϕ_{0d} coefficient, which reflects NADH release in the dismutation reaction, contains three different terms $\{\phi_{0u}(1+[B]/K_{aiS})+\phi_B\phi_Q/\phi_{SQ}\}$, where the last term and the $\phi_{0u}(1+[B]/K_{aiS})$ term can be precisely estimated from the inhibition experiments. To accomplish this, pyrazole was used as an inhibitor with varied NAD^+, as it only formed an EAI and an EBI complex. The intercept of the double inverse plot obtained at 6 mM acetaldehyde is $\phi_{0d}+\phi_{Bd}/[B]$, and as pyrazole forms an EAI complex with a $K_{EA,I}$ value of 4.4 μM (Table 3), the two ϕ_{Bd} terms should be multiplied by $(1+[I]/K_{EA,I})$. The formation of an EBI complex affects the terms derived from the free enzyme, ϕ_Q and ϕ_{SQ}. However, this inhibition complex can be neglected as the two ϕ terms are equally affected. $\phi_B\phi_Q/\phi_{SQ}$ was estimated to be 3.4 s and $\phi_{0u}(1+[B]/K_{aiS})$ to be 0.4 s, and hence ϕ_{0u} must be less than 0.4 s. If it is assumed that k_5 approximates k_{10} then K_{aiS} equals K_{iS} (Table 1). If we use the previously determined value of 9.5 mM for K_{iS} [16] and 6.0 mM for [B], ϕ_{0u} becomes 0.25 s. This would indicate that under initial-rate conditions, 0.25 molecules of NADH were released ($1/\phi_{0d}$) and 4 molecules of acetate were produced per enzyme active site per second. From NMR studies with large amounts of Adh, combined with spectroscopic rate measurements, Henehan et. al. [8] estimated the acetate/NADH ratio under approximate initial-rate conditions to be >20. Although this is probably an overestimation, it is close to the value of 16 now obtained with the approximation that k_5 and k_{10} are similar.

Previously the ϕ_{SQ}/ϕ_Q value was determined to be 1.51 [14] and <2.55 mM [16] from acetaldehyde reduction and product-inihibition studies respectively. The determination of ϕ_{SQ} and ϕ_Q at basic pH [14] is uncertain due to the low sensitivity of the spectrophotometric method used. As $\phi_B\phi_Q/\phi_{SQ}$ was estimated to be 3.4 s and the ϕ_B value to be 6.6 mM s, the ϕ_{SQ}/ϕ_Q value was calculated to be 1.9 mM. This value fits well with our previously determined values. In the different inhibition studies with varied NAD^+, the fixed acetaldehyde concentration was either 6.0 or 0.67 mM. Based on the estimated ϕ_{ABd} coefficient of 0.106 mM^2 s, the ϕ_{Ad} coefficient was calculated to be 60 μM s. Table 1 shows that the ϕ_{Ad} coefficient contains two terms, ϕ_A, which reflects the binding of NAD^+ to the free enzyme, and $\phi_{AB}\phi_Q/\phi_{SQ}$. Using a ϕ_Q/ϕ_{SQ} value of 0.5 mM^{-1} and a ϕ_{AB} value of 0.106 mM^2 s, ϕ_A was calculated to be 7 μM s. This fits with the previously published constant of 6 μM s from ethanol oxidation [14].

Previous studies showed that both coenzymes bind to the free enzyme, and product-inihibition studies with NADH gave a K_{iq} of 3.7–3.8 μM (Table 3). In the oxidation of acetaldehyde, NADH is a competitive inhibitor with respect to NAD^+, which shows that the two coenzymes bind to the same enzyme form. The inhibition constant obtained for NADH with varied NAD^+ and a fixed acetaldehyde concentration is not the same for the dismutation mechanism in Scheme 1 (K_{is} or K_{iqd}) as the K_{iq} obtained from an ordinary unbranched pathway, due to the reaction of acetaldehyde with the EQ complex formed (eqn. 4 and Table 1). The K_{iqd} value obtained is therefore much lower than the K_{iq} value, as seen in Table 3. This resulted in correction factors f_1 and f_2 (Table 1) of 0.03 and 43 respectively, at the acetaldehyde concentration used.

Kinetic isotope effects and substrate specificity

Studies of acetaldehyde and 1-[$^2H_1$]acetaldehyde revealed a kinetic isotope effect of 3.4 on $(k_{cat}/K_m)^H/(k_{cat}/K_m)^{2H}$ (Table 2). Similar isotope effects were observed with ethanol, propan-2-ol and cyclohexanol [28]. These isotope effects result from the fact that in a compulsory ordered mechanism, the k_{cat}/K_m or $1/\phi_B$ term contains the rate constant for the hydride-transfer step [30]. To simplify the analysis of Scheme 1, this step has been omitted since it does not influence the outcome of the analysis. However, no primary isotope effect was obseved for $k_{cat}{}^H/k_{cat}{}^{2H}$ with the two aldehydes (Table 2), although the $\phi_B\phi_Q/\phi_{SQ}$ term accounts for approximately 90 % of the ϕ_{0d} value and $\phi_{0u}(1+[B]/K_{aiS})$ for only 10 %. The ϕ_{SQ} term also contains the rate constant for the hydride-transfer step, i.e. those for the lower pathway in Scheme 1. As the stereochemistry at the nicotinamide ring is the same in the oxidation of alcohols and aldehydes (J.-O. Winberg, J. S. Svendsen and J. S. McKinley-McKee, unpublished work), the

deuterium in the NADH formed is transferred to ethanol during the dismutation reaction. As both the ϕ_B and ϕ_{SQ} terms involve the rate constant for the hydride-transfer steps, these two terms balance out the isotope effect or even account for the slightly larger k_{cat} of the deuterated substrate. If there is an isotope effect on the ϕ_{0u} term, this effect can be masked due to the low contribution of ϕ_{0u} to the ϕ_{0d} term and a possible inverse isotope effect on the $\phi_B\phi_Q/\phi_{SQ}$ term. Therefore it is not possible to decide whether there is an isotope effect on the ϕ_{0u} term or not, and hence, if the conversion of the ternary EAB into EQP is involved in the rate-limiting step of the reaction.

The substrate specificity or 'on' velocity coefficient $k_{cat}/K_m(1/\phi_D)$ is 0.4 and 9.0 $mM^{-1}\cdot s^{-1}$ for ethanol and propan-2-ol respectively [14,22]. Table 2 shows this coefficient for aldehydes for which no correction has been made for the *gem*-diol content. In the oxidation of the aldehydes to their corresponding carboxylic acids, the *gem*-diol form of the aldehydes may bind to the same site in the EA complex as an alcohol, and hence mimic the binding of a secondary alcohol, as previously suggested by Eisses [7]. Even if corrected for the *gem*-diol content, the substrate-specificity constant for acetaldehyde is still smaller than for ethanol. Thus, the enzyme–NAD^+ complex reacts more slowly with acetaldehyde than with ethanol and propan-2-ol. This corresponds with previous studies on the substrate (alcohol) specificity of *Drosophila* Adhs, from which it was concluded that the alcohol binding site in *Drosophila* Adh was hydrophobic and preferred non-polar and non-charged side-chains [3]. These studies also showed that a branch at the C-2 position of primary alcohols and the C-3 position of secondary alcohols reduced the k_{cat}/K_m value compared with the unbranched parent alcohol [3]. In the case of secondary alcohols, it was also shown that the reduction in k_{cat}/K_m was less for *S*-enantiomers due to a presumed wider *R*-2 binding pocket. By correcting for the *gem*-diol content of the aldehydes investigated, the ratio of k_{cat}/K_m for trimethylacetaldehyde to k_{cat}/K_m for acetaldehyde was 1.8 for the diol forms, 0.3 for the carbonyl forms and 0.6 for the mixture. Based on this, it is tempting to assume that both forms of an aldehyde can bind to the active site of the enzyme. In the case of the carbonyl form, an enzyme-catalysed hydration of the aldehyde might occur before hydride transfer, as is suggested to occur in the oxidation of benzaldehyde with horse liver Adh [33].

Concluding remarks

Will an aldehyde produced during the oxidation of an alcohol compete with the alcohol oxidation under initial-rate conditions and hence prevent reliable results for the oxidation reaction? The answer is no, as the amount of acetaldehyde produced in the oxidation of ethanol under initial-rate conditions is in the region of 0.1–1 μM in fluorimetric assays and 1–10 μM in spectrophotometric assays. Even with a sensitive recording fluorimeter, as in the present work, and an enzyme concentration approximately 10 times that in an ethanol oxidation assay, it is not possible to detect any NADH production at acetaldehyde concentrations below 0.1 mM. Likewise, the alcohol produced during the dismutation reaction is also too small to affect the aldehyde oxidation and NADH produced, even if the acetate production, and hence the alcohol production, is 10–20 times the NADH produced, i.e. maximum 0.01–0.02 mM, which is far below the K_m value of 3.4 mM for ethanol [14].

It can be concluded that even if the NADH release is small compared with the acetate and ethanol production in the dismutation reaction at high pH, the kinetic coefficients obtained through the determination of NADH production under initial-rate conditions can be used to determine both the substrate specificity and the overall reaction mechanism. Even though it is only possible to measure NADH release above pH 9 [8], it is reasonable to assume that the substrate specificity determined at pH 9.5 is also valid at other pHs. This is based on our previous studies of alcohol specificity for this enzyme, which showed that ϕ_D varied with pH, but the variation was identical for different alcohols [14].

Received 10 April 1997/16 September 1997; accepted 23 September 1997

REFERENCES

1 Chambers, G. K. (1988) Adv. Genet. **25**, 39–107
2 Chambers, G. K. (1991) Comp. Biochem. Physiol. B: Biochem. Mol. Biol. **99**, 723–730
3 Winberg, J. O. and McKinley-McKee, J. S. (1992) Int. J. Biochem. **24**, 169–181
4 Heinstra, P. W. H., Eisses, K.Th., Schoonen, W. G. E. J., Aben, W., de Winter, A. J., van der Horst, D. J., van Marrevijk, W. J. A., Beenakkers, A. M. Th., Scharloo, W. and Thörig, G. E. W. (1983) Genetica **60**, 129–137
5 Moxon, L. N., Holmes, R. S., Parsons, P. A., Irving, M. G. and Doddrell, D. M. (1985) Comp. Biochem. Physiol. B: Biochem. Mol. Biol. **80**, 525–535
6 Eisses, K.Th., Schoonen, W. G., Aben, W., Scharloo, W. and Thörig, G. E. W. (1985) Mol. Gen. Genet. **199**, 76–81
7 Eisses, K.Th. (1989) Bioorg. Chem. **17**, 268–274
8 Henehan, G. T. M., Chang, S. H. and Oppenheimer, N. J. (1995) Biochemistry **34**, 12294–12301
9 Jörnvall, H., Persson, B. and Jeffery, J. (1981) Proc. Natl. Acad. Sci. U.S.A. **78**, 4226–4230
10 Jörnvall, H., Persson, B., Krook, M. and Kaiser, R. (1990) Biochem. Soc. Trans. **18**, 169–171
11 Chen, Z., Lu, L., Shirley, M., Lee, W. R. and Chang, S. H. (1990) Biochemistry **29**, 1112–1118
12 Chen, Z., Jiang, J. C., Lin, Z.-G., Lee, W. R., Baker, M. E. and Chang, S. H. (1993) Biochemistry **32**, 3342–3346
13 Cols, N., Marfany, G., Atrian, S. and Gonzalez-Duarte, R. (1993) FEBS Lett. **319**, 90–94
14 Winberg, J. O. and McKinley-McKee, J. S. (1988) Biochem. J. **255**, 589–599
15 McKinley-McKee, J. S., Winberg, J. O. and Pettersson, G. (1991) Biochem. Int. **25**, 879–885
16 Winberg, J. O. and McKinley-McKee, J. S. (1994) Biochem. J. **301**, 901–909
17 Winberg, J. O. and McKinley-McKee, J. S. (1988) Biochem. J. **251**, 223–227
18 Heinstra, P. W. H., Geer, B. W., Seykens, D. and Langevin, M. (1989) Biochem. J. **259**, 791–797
19 Dalziel, K. and Dickinson, F. M. (1965) Nature (London) **206**, 255–257
20 Hinson, J. A. and Neal, R. A. (1972) J. Biol. Chem. **247**, 7106–7115
21 Thatcher, D. R. (1980) Biochem. J. **187**, 875–886
22 Winberg, J. O., Hovik, R. and McKinley-McKee, J. S. (1985) Biochem. Genet. **23**, 205–216
23 Theorell, H. and Nygaard, A. P. (1954) Acta Chem. Scand. **8**, 877–888
24 Theorell, H. and McKinley-McKee (1961) Acta Chem. Scand. **15**, 1797–1810
25 Kaplan, N. (1960) Enzymes 3rd Ed. **3**, 105–169
26 Oppenheimer, N. J. (1987) In Pyridine Nucleotide Enzymes, Part A (Dolfin, D., Arramoric, O. and Poulson, R., eds.), pp. 323–365, Wiley, New York
27 Winberg, J. O., Thatcher, D. R. and McKinley-McKee, J. S. (1982) Biochim. Biophys. Acta. **704**, 17–25
28 Hovik, R., Winberg, J.-O. and McKinley-McKee, J. S. (1984) Insect Biochem. **14**, 345–351
29 Winberg, J. O., Hovik, R., McKinley-McKee, J. S., Juan, E. and Gonzalez-Duarte, R. (1986) Biochem. J. **235**, 481–490
30 Dalziel, K. (1957) Acta Chem. Scand. **11**, 1706–1723
31 Cleland, W. W. (1977) In Advances in Enzymology, Vol. 45 (Meister, A., ed.), pp. 273–387, John Wiley, New York
32 Dixon, M., Webb, E. E., Thorne, C. J. R. and Tipton, K. F. (1979) Enzymes, 3rd Ed., 103–105
33 Olsen, L. P., Luo, J., Almarsson, Ö. and Bruice, T. C. (1996) Biochemistry **35**, 9782–9791
34 Cleland, W. W. (1963) Biochim. Biophys. Acta, **67**, 104–137
35 Cleland, W. W. (1963) Biochim. Biophys. Acta, **67**, 173–187
36 Fromm, H. J. (1975) Initial Rate Enzyme Kinetics (Kleinzeller, A., Springer, G. F. and Wittmann, H. G., eds.), pp. 33–36, Springer Verlag, Berlin, Heidelberg and New York